HHS Public Access

Author manuscript

J Nutr Biochem. Author manuscript; available in PMC 2019 May 01.

Published in final edited form as:

J Nutr Biochem. 2018 May ; 55: 157–164. doi:10.1016/j.jnutbio.2018.02.005.

Raspberry promotes brown and beige adipocyte development in mice fed high-fat diet through activation of AMP-activated protein kinase (AMPK) α1

Tiande Zou[1,2], **Bo Wang**[2], **Qiyuan Yang**[2], **Jeanene M. de Avila**[2], **Mei-Jun Zhu**[3], **Jinming You**[1], **Daiwen Chen**[4], and **Min Du**[2,5,*]

[1]Jiangxi Province Key Laboratory of Animal Nutrition, Engineering Research Center of Feed Development, Jiangxi Agricultural University, Nanchang 330045, Jiangxi, China

[2]Laboratory of Nutrigenomics and Growth Biology, Department of Animal Sciences, Washington State University, Pullman, WA 99164, USA

[3]School of Food Sciences, Washington State University, Pullman, WA 99164, USA

[4]Animal Nutrition Institute, Sichuan Agricultural University, Chengdu 611130, Sichuan, China

[5]Beijing Advanced Innovation Center for Food Nutrition and Human Health, College of Food Science & Nutritional Engineering, China Agricultural University, Beijing 100194, China

Abstract

Development of brown and beige/brite adipocytes increases thermogenesis and helps to reduce obesity and metabolic syndrome. Our previous study suggests that dietary raspberry can ameliorate metabolic syndromes in diet-induced obese mice. Here, we further evaluated the effects of raspberry on energy expenditure and adaptive thermogenesis and determined whether these effects were mediated by AMP-activated protein kinase (AMPK). Mice deficient in the catalytic subunit of AMPKα1 and wild-type (WT) mice were fed a high-fat diet (HFD) or HFD supplemented with 5% raspberry (RAS) for 10 weeks. The thermogenic program and related regulatory factors in adipose tissue were assessed. RAS improved the insulin sensitivity and reduced fat mass in WT mice but not in AMPKα1$^{-/-}$ mice. In the absence of AMPKα1, RAS failed to increase oxygen consumption and heat production. Consistent with this, the thermogenic gene expression in brown adipose tissue and brown-like adipocyte formation in subcutaneous adipose tissue were not induced by RAS in AMPKα1$^{-/-}$ mice. In conclusion, AMPKα1 is

*Corresponding Author: Min Du, Ph.D., Washington Center for Muscle Biology, Department of Animal Sciences, Washington State University, Pullman, WA 99164; Tel: 509-335-2744; Fax: 307-766-2355; min.du@wsu.edu.

Author contributions

T.Z. and M.D. conceived the project, designed the experiments, analyzed data and wrote the manuscript. T.Z., B.W. and Q.Y. performed the experiments. J.M.A. assisted with the mouse experiments and metabolic rate analyses. M.J.Z., J.Y. and D.C. contributed to the discussion and reviewed and edited the manuscript.

Conflicts of interest

The authors declare no conflict of interest.

indispensable for the effects of RAS on brown and beige/brite adipocyte development, and prevention of obesity and metabolic dysfunction.

Keywords

AMP-activated protein kinase (AMPK) α1; Browning; Obesity; Raspberry; Thermogenesis

Introduction

The prevalence of obesity is increasing rapidly worldwide and is recognized as a major risk factor leading to metabolic diseases such as type 2 diabetes, cancer and cardiovascular disease [1, 2]. Adipose tissues have been considered as master regulators of energy homeostasis. In mammals, white adipose tissue (WAT) is the major site of excess energy storage in the form of triglycerides [3]. Differently, two populations of uncoupling protein 1 (UCP1)-expressing thermogenic adipocytes, called classical brown adipocytes from brown adipose tissue (BAT) and brite/beige (**br**own in wh**ite**) adipocytes from WAT, dissipate energy as heat through non-shivering thermogenesis [3, 4]. The amounts of thermogenic brown/beige adipocytes are inversely correlated with obesity in adult humans [5]. Thus, pharmacologic or nutritional enhancement of BAT development and thermogenic activity and browning of WAT may be one of the most promising strategies to counteract obesity and metabolic disease [6].

Raspberry (RAS), a fruit enriched with polyphenols of high digestibility, has been shown to ameliorate high-fat diet-induced obesity and the accompanying metabolic dysfunction in mammals [7, 8] and exert health-beneficial effects [9–11]. In addition, fruit polyphenolic compounds are known to prevent obesity by promoting thermogenic program in BAT and WAT and inducing beige adipocyte development within WAT [12, 13]. Although RAS has preventive or therapeutic effects on diet-induced obesity, little is known about the role of RAS on the formation and function of brown and beige adipocytes.

AMP-activated protein kinase (AMPK) is a key regulator of cell metabolism, composed of α, β and γ subunits [14]. The catalytic subunit of AMPK has two isoforms, α1 and α2, which display different tissue expression patterns. The α1 isoform is prominently expressed in progenitor cells and adipose tissue [15], whereas the α2 subunit is the predominant isoform expressed in muscle [16]. Moreover, we previously found that AMPKα1 participates in resveratrol stimulated brown and beige adipogenesis [13, 17]. Here, we hypothesized that RAS regulates adaptive thermogenesis through promoting brown adipocyte function and white adipocyte browning, a process mediated by AMPKα1. Thus, the objective of the present study is to investigate the effects of RAS supplementation of high-fat diet-fed mice on BAT metabolic function and browning of WAT and to explore the role of AMPKα1 in mediating the beneficial effects of dietary RAS.

Materials and methods

Animal, diet and experimental design

All animal experimental and care procedures were conducted in accordance with the guidelines of the National Institutes of Health and approved by the Animal Use and Care Committee of Washington State University (Permit No. 04719). To achieve AMPKα1 conditional knockout, AMPKα1$^{flox/flox}$ C57BL/6 mice (Stock No: 014141, Jackson Lab, Bar Harbor, Maine) were cross-bred with tamoxifen-inducible Rosa-Cre C57BL/6 mice (Stock No: 004847, Jackson Lab) to generate Rosa^{Cre}/AMPKα1$^{flox/flox}$. Breeding was performed in house. Rosa^{Cre}/AMPKα1$^{flox/flox}$ mice were injected intraperitoneally with tamoxifen (75 μg/g body weight) for 4 continuous days to induce AMPKα1 knockout (AMPKα1$^{-/-}$, α1KO) [18, 19]. To avoid possible tamoxifen effect on brown/beige adipogenesis [20], AMPKα1$^{flox/flox}$ mice treated with tamoxifen were used as controls (Wild-type, WT); as previously characterized, the Rosa-Cre gene does not affect brown/beige adipogenesis [21]. Mice were allowed to rest for at least 3 days after the last tamoxifen injection before dietary treatments in order to minimize possible confounding changes.

Wild-type and AMPKα1$^{-/-}$ C57BL/6 male mice (2 months old) were fed a high-fat diet (HFD; 60% energy from fat, D12492; Research Diets, New Brunswick, NJ, USA) or a HFD diet supplemented with freeze dried raspberry (5% of dry feed weight, red raspberry powder) for 10 weeks (n = 6 per group). To prepare raspberry diet, organic frozen red raspberries were purchased from a local Safeway supermarket (Pullman, WA), originally distributed by Lucerne Foods, Inc. (Boise, ID, USA). RAS were freeze-dried using VirTis freeze drier (Vertis, Gardiner, NY, USA) and ground into powder. The RAS powder contains 1.09 ± 0.05% gallic acid equivalent polyphenolics, 4.24 ± 0.12% protein, 1.91 ± 0.03% fat, 0.81 ± 0.02% ash, and 16.14 ± 0.45% moisture. According to a recent publication, freeze-dried RAS contains 35.1% dietary fiber, in which soluble fiber is 1.6 ± 0.2% and insoluble fiber is 33.5 ± 0.1% [9]. The RAS powder was shipped to the Research Diets, Inc. for making customized research diets containing 5% of RAS on dry weight basis [7]. Diets were vaccum-packaged and frozen in −80 °C until used and fresh diets were provided weekly. We chose 5% RAS supplementation, because dietary supplementation of 5% RAS effectively ameliorated HFD-induced adiposity [7]. Mice were maintained in a temperature-controlled conditions (23 ± 2 °C, 12:12-h light-dark cycle) with free access to food and water. Feed intake and body weight were monitored weekly during dietary treatments. After 10 weeks of treatments, mice were euthanized by carbon dioxide anesthesia followed by cervical dislocation. Blood samples were collected by cardiac puncture and centrifuged at 4°C to collect serum. The interscapular BAT, inguinal WAT (IngWAT) and epididymal WAT (EpiWAT) were rapidly isolated and weighed. Tissues from one side were fixed in 4% paraformaldehyde for sectioning and staining, and from the other side, they were rapidly frozen in liquid nitrogen and stored at −80°C until further analysis. A portion of IngWAT was used for tissue oxygen consumption measurement.

Glucose tolerance test (GTT)

At 1 week before the mice were killed, following an overnight fasting, mice were i.p. injected with D-glucose (2 g/kg). Blood samples were collected from the tail vein at 0, 15,

30, 60 and 90 min after injection and glucose concentrations were measured using a glucometer (Bayer Contour, Tarrytown, NY, USA), and the area under the curve was quantified [19, 22].

Serum analysis

The content of serum free fatty acids was determined using an EnzyChrom™ Free Acid Assay Kit (BioAssay System, CA, USA). Serum triglyceride and total cholesterol levels were measured using colourimetric assay kits (Thermo-Scientific, Ann Arbor, MI, USA). Serum insulin concentration was measured using a Mouse Ultrasensitive Insulin ELISA Kit (ALPCO Diagnostics, Salem, NH, USA).

Whole-body metabolic analysis

The whole-body metabolic rate [oxygen consumption (VO_2), carbon dioxide production (VCO_2), respiratory exchange ratio (RER) and heat production] of mice during the day (quiescent stage) and night (active stage) was measured using an Oxymax indirect open-circuit calorimetry system (Columbus Instruments, Columbus, OH, USA) installed in a constant environmental temperature and light regimen (12 h light and 12 h dark). Mice in each chamber had free access to food and water.

Oxygen consumption assay

IngWAT was isolated, weighed, and 50 mg of tissue was minced in a respiration buffer (2% BSA, 1.1 mM sodium pyruvate, and 25 mM glucose in PBS). Oxygen consumption was measured using an Orion 3-Star Dissolved Oxygen Meter (Thermo Scientific, Waltham, MA, USA) for approximately 25 min. Oxygen consumption was normalized to minced tissue weight [23].

Histological analysis

Paraffin-embedded WAT and BAT sections (5-μm thick) were either stained with Hematoxylin and Eosin (H&E) or used for UCP1 immunohistochemical (IHC) staining as previously described [24]. Imaging was performed with an EVOS microscope (Advanced Microscopy Group, Bothell, WA, USA). At least four images per section and four sections from each individual mouse were analyzed. Adipocyte diameters were measured by Image-Pro Plus 6.0 (Media Cybernetics, Inc., Rockville, MD, USA).

Quantitative real-time PCR (qRT-PCR) analysis

Total RNA was extracted from adipose tissues by TRIzol reagent (Sigma, Saint Louis, MO, USA), and cDNA was synthesized with the iScriptTM cDNA Synthesis Kit (Bio-Rad, Hercules, CA, USA). qRT-PCR was carried out on the CFX RT-PCR detection system (Bio-Rad) with 18S rRNA used as a reference gene as described previously [13]. Relative expression of mRNA was determined using the method of $2^{-\Delta\Delta Ct}$ [25]. The primer sequences are shown in Table 1.

Immunoblotting analysis

Immunoblotting analyses were performed as previously described [24]. Briefly, protein samples were extracted from adipose tissues and separated by 10% SDS-PAGE followed with nitrocellulose membrane transferring. After blocking in a blocking solution consisting of 5% nonfat dry milk in TBS with 0.1% Tween 20 (TBST), membranes were overnight incubated with the selected primary antibodies at 4 °C, followed by incubation with either IRDye 800CW goat anti-rabbit or IRDye 680 goat anti-mouse secondary antibodies at room temperature for 60 min. Finally, membranes were visualized using the Odyssey Infrared Image System (LI-COR Biosciences, Lincoln, NE, USA). Band density of target protein was quantified and then normalized to β-tubulin content. UCP1 and PR domain-containing 16 (PRDM16) polyclonal antibodies were purchased from Thermo Scientific (Waltham, MA, USA) and were diluted 1:1000. Antibodies against cytochrome *c* (Cyto C), AMPKα, phosphorylated-AMPKα (p-AMPKα) at Thr172 and β-tubulin were purchased from Cell Signaling (Danver, MA, USA) and were diluted 1:1000. IRDye 800CW goat anti-rabbit and IRDye 680 goat anti-mouse secondary antibodies were purchased from LI-COR (Lincoln, NE, USA) and were diluted 1:15,000.

Statistical analysis

All data sets were normally distributed, thus, the general linear model and Duncan's multiple range test were used to analyze the data and to determine the significance of differences among means of different treatments, using SAS 9.0 (SAS Institute Inc., Cary, NC, USA). Results are expressed as mean ± SEM. A significant difference was considered as $P < 0.05$.

Results

Raspberry does not reduce body weight gain and adiposity in AMPKα1$^{-/-}$ mice

The average weekly food intake was similar for WT and AMPKα1$^{-/-}$ mice and was not affected significantly by RAS (Fig. 1A). Dietary RAS supplementation reduced the body weight of WT mice but not that of AMPKα1$^{-/-}$ mice (Fig 1. B and C). Consistently, RAS increased the BAT mass (Fig. 1D, $P = 0.037$) and decreased the IngWAT ($P = 0.011$) and EpiWAT ($P = 0.016$) mass (Fig. 1E) in WT mice. These data showed that AMPKα1 might be required for the anti-obesity effect of RAS.

Raspberry does not improve insulin sensitivity in AMPKα1$^{-/-}$ mice challenged with HFD

To investigate the role of AMPKα1 deficiency on obesity-associated insulin resistance, we determined the metabolic parameters of WT and AMPKα1$^{-/-}$ mice challenged with HFD. Glucose tolerance was similar between WT and AMPKα1$^{-/-}$ mice on HFD alone. However, glucose tolerance was improved by RAS in WT mice but not in AMPKα1$^{-/-}$ mice (Fig. 2A). RAS reduced the contents of serum free fatty acids (Fig. 2B, $P = 0.008$), triglycerides (Fig. 2C, $P = 0.008$), cholesterol (Fig. 2D, $P = 0.014$) and insulin (Fig. 2E, $P = 0.001$) in WT mice but not in AMPKα1$^{-/-}$ mice. These results suggested that RAS-induced improvements in metabolic homeostasis requires AMPKα1.

Raspberry does not increase whole-body energy expenditure in AMPKα1$^{-/-}$ mice challenged with HFD

To explore why AMPKα1$^{-/-}$ mice on RAS did not lose weight, we measured their whole-body energy expenditure. The O_2 consumption (Fig. 3A and B) and CO_2 production (Fig. 3C and D) during light and dark phases were increased by RAS in WT mice but not in AMPKα1$^{-/-}$ mice. As a result, the increased RER was decreased by RAS in WT mice but not in AMPKα1$^{-/-}$ mice (Fig. 3E and F), suggesting RAS-induced lipid oxidation required AMPKα1. Furthermore, consistent with O_2 consumption, RAS increased the heat production in WT mice but not in AMPKα1$^{-/-}$ mice (Fig. 3G and H).

To analyze the impact of RAS on adipose tissue, IngWAT was separated for direct O_2 consumption analysis. Consistently, RAS increased the basal O_2 consumption in IngWAT of WT mice (Fig. 3I, $P = 0.048$). However, RAS did not increase the basal O_2 consumption of IngWAT in AMPKα1$^{-/-}$ mice *in vitro*. Taken together, these results showed that RAS-induced improvements in metabolic activity required AMPKα1.

Raspberry does not increase BAT metabolic activity in AMPKα1$^{-/-}$ mice challenged with HFD

To determine the source of the increased energy expenditure in WT mice treated with RAS, we measured BAT metabolic function in these mice. Histological analysis showed that RAS reduced lipid deposits and increased UCP1 expression in BAT of WT mice. However, the morphology and UCP1 protein staining were not affected by RAS in BAT of AMPKα1$^{-/-}$ mice (Fig. 4A). Consistent with these findings, RAS increased the UCP1 mRNA (Fig. 4B, $P = 0.008$) and protein expression (Fig. 4C and D, $P = 0.017$) in BAT of WT mice but not in AMPKα1$^{-/-}$ mice. Correspondingly, the mRNA expression of PRDM16 ($P = 0.008$), peroxisomal proliferator-activated receptor γ coactivator-1 α (PGC-1α, $P = 0.012$), cell death-inducing DFFA-like effector A (Cidea, $P = 0.026$) and cytochrome c oxidase subunit Vlla polypeptide 1 (Cox7al, $P = 0.011$) were also increased by RAS in WT mice but not in AMPKα1$^{-/-}$ mice (Fig. 4B). In addition, RAS increased p-AMPKα protein content in BAT of WT mice but not that of AMPKα1$^{-/-}$ mice (Fig. 4C and D, $P = 0.046$). A similar pattern of changes was observed for PRDM16 and cytochrome c (Cyto C) in WT mice but absence in AMPKα1$^{-/-}$ mice (Fig. 4C and D). These data provide evidence that RAS-induced improvements in BAT thermogenic activity require AMPKα1.

Raspberry does not induce brown fat-like changes in WAT of AMPKα1$^{-/-}$ mice challenged with HFD

Besides BAT activity, browning of WAT is another important process in adaptive thermogenesis. H&E staining results revealed that the average adipocyte diameters were decreased by RAS in WAT of WT mice but not in AMPKα1$^{-/-}$ mice (Fig. 5A). Small adipocytes were most abundant in WT mice treated with RAS (Fig. 5B and C). Moreover, beige adipocyte numbers (Fig. 5A) and UCP1-positive areas (Fig. 5D) were increased by RAS in IngWAT of WT mice but not in AMPKα1$^{-/-}$ mice. However, RAS did not affect the beige adipocyte formation (Fig. 5A) and UCP1 protein staining (Fig. 5D) in EpiWAT of both WT mice and AMPKα1$^{-/-}$ mice, which implies that EpiWAT might be not sensitive enough to browning-associated stimuli. Correspondingly, UCP1 mRNA (Fig. 5E, $P = 0.005$) and

protein expression (Fig. 5F and G, $P = 0.014$) were also increased by RAS in IngWAT of WT mice but not in AMPKα1$^{-/-}$ mice. RAS increased the expression of a series of thermogenic genes in IngWAT of WT mice but not in AMPKα1$^{-/-}$ mice, including PRDM16 ($P = 0.022$), PGC-1α ($P = 0.032$) and elongation of very long-chain fatty acids protein 3 (Elovl3, $P = 0.019$) (Fig. 5E). Moreover, RAS also induced the mRNA expression of beige adipocyte-selective markers in IngWAT of WT mice, including cluster of differentiation 137 (CD137, $P = 0.036$), T-box1 (Tbx1, $P = 0.049$) and transmembrane protein 26 (Tmem26, $P = 0.004$) (Fig. 5E). However, RAS did not affect the mRNA expression of these genes in IngWAT of AMPKα1$^{-/-}$ mice (Fig. 5E). In addition, PRDM16 ($P = 0.011$) and Cyto C ($P = 0.037$) protein contents were increased by RAS in IngWAT of WT mice but not in AMPKα1$^{-/-}$ mice (Fig. 5F and G). A similar pattern of changes was observed for p-AMPKα (Fig. 5F and G). These results suggested that RAS-induced IngWAT browning requires AMPKα1.

Discussion

The imbalance between energy intake and energy expenditure induces animal overweight and obesity leading to metabolic diseases [26]. The development and thermogenic function of BAT plays an important role in an adequate neonatal response to prevent hypothermia. BAT burns fatty acids and glucose for heat production and is able to produce 300 times more heat than other tissues per unit mass [27]. Thus, brown and beige adipose tissues have been identified as promising therapeutic targets against diet-induced obesity and diabetes [28]. RAS, which contains high contents of both polyphenols and dietary fibers, has shown to be beneficial for the prevention and treatment of obesity and related chronic diseases including diabetes, oxidative stress and heart diseases [8, 9, 29, 30]. In our previous studies, we observed that RAS ameliorates adiposity and metabolic syndromes in diet-induced obese mice [7]. However, to our knowledge, no study assessed RAS's effects on brown and beige adipogenesis and thermogenesis. In the present study, we used the HFD-induced obesity mice model to investigate the effects of RAS on BAT/beige adipocyte function and thermogenesis and explored the underlying mechanism. Our results showed that RAS increased energy expenditure and adaptive thermogenesis by promoting BAT metabolic activity and beige adipocyte formation through the activation of AMPKα1.

It has been reported that increased energy expenditure contributes to body weight loss and protects against diet-induced obesity [31]. As determined by an indirect calorimetry, in our study, the increased metabolic rate and decreased fat mass induced by RAS are related, at least partly, to the increased whole-body energy expenditure. More importantly, after AMPKα1 knockout, the promotional effects of RAS on the oxygen consumption and heat production were abolished. In accordance, our *in vitro* data further suggested RAS fails to increase the basal oxygen consumption of IngWAT in AMPKα1$^{-/-}$ mice. The RER is commonly used to analyze the sources of fuel. A high RER suggests that carbohydrates are being predominantly utilized, whereas a low RER indicates fatty acid oxidation [32]. In this study, the decreased RER in RAS-treated WT mice suggests that a higher ratio of lipids was being oxidized. Together, these findings suggest that AMPKα1 mediates RAS-induced energy expenditure.

Enhanced BAT metabolic function and browning of IngWAT could lead to increased oxygen consumption and heat production. The differentiation and function of brown/beige adipocytes are regulated by a complex network of transcription factors and signaling pathway components. PRDM16 is a crucial transcription factor in brown and beige adipogenesis [33]. The expression of PRDM16 results in up-regulation of genes involved in BAT/beige adipocyte function and thermogenesis, including UCP1, PGC-1α and Cyto C [34, 35]. AMPK, an important energy sensor, mediates dietary polyphenols-induced anti-obesity effects [13, 24]. In our previous studies, we found that AMPK promotes PRDM16 expression [21], and resveratrol, a representative polyphenol present in grape and some berries, activates AMPK [13]. To evaluate the possibility that RAS, which contains a high level of polyphenols, activates AMPKα1 for brown/beige fat activation, we studied the effects of RAS in mice deficient in AMPKα1. As expected, only trace amount of p-AMPKα was detected in BAT and IngWAT of AMPKα1$^{-/-}$ mice, suggesting that α1 isoform accounts for most of the total AMPKα activity. More importantly, RAS increased the phosphorylated AMPKα level in WT mice and RAS-induced increase of the expression of PRDM16 and other thermogenic genes in BAT and IngWAT are abolished after knockout of AMPKα1, showing that the biological effects of RAS on BAT metabolic function and browning of IngWAT are largely mediated through AMPKα1.

Based on lineage tracing, brown adipocytes are derived from MYF5 (myogenic factor 5)-expressing cells [36], whereas most of the beige adipocytes in WAT are developed from platelet-derived growth factor receptor α positive (PDGFRα^{+}) cells [37, 38]. The density of progenitor cells varies among different fat depots. Compared with EpiWAT, IngWAT possesses higher density of PDGFRα^{+} progenitor cells and higher expansion capacity, and may be more sensitive to browning-associated stimuli [22, 39]. The low density of PDGFRα^{+} progenitor cells in EpiWAT limits *de novo* formation of beige adipocytes, which might explain the lack of changes in EpiWAT beige adipogenesis of both WT mice and AMPKα1$^{-/-}$ mice, due to new beige adipocytes are mainly derived from PDGFRα^{+} progenitor cells [40].

In conclusion, we have demonstrated that RAS promotes a thermogenic program in BAT and WAT in HFD-fed mice by stimulating the expression of thermogenic genes and beige adipocyte formation, which are mediated by AMPKα1. This study provides new insights into the regulation of brown/beige adipocyte formation and thermogenesis by dietary RAS and suggests the potential application of RAS as a nutritional intervention strategy for the prevention and therapeutic of obesity and related metabolic diseases.

Acknowledgments

This study was supported by grants from the National Institutes of Health (R01-HD067449 and R21-AG049976) and a grant from the National Processed Raspberry Council to M.D.

Abbreviations

AMPK	AMP-activated protein kinase
BAT	brown adipose tissue

CD137	cluster of differentiation 137
Cidea	cell death-inducing DFFA-like effector A
Cox7al	cytochrome c oxidase subunit Vlla polypeptide 1
Cyto C	cytochrome c
Elovl3	elongation of very long-chain fatty acids protein 3
EpiWAT	epididymal white adipose tissue
GTT	glucose tolerance test
HFD	high-fat diet
IngWAT	inguinal white adipose tissue
PGC-1α	peroxisomal proliferator-activated receptor γ coactivator-1
PRDM16	PR domain-containing 16
RAS	raspberry
RER	respiratory exchange ratio
Tbx1	T-box 1
Tmem26	transmembrane protein 26
UCP1	uncoupling protein 1

References

1. Ding J, Reynolds LM, Zeller T, Müller C, Lohman K, Nicklas BJ, et al. Alterations of a Cellular Cholesterol Metabolism Network Are a Molecular Feature of Obesity-Related Type 2 Diabetes and Cardiovascular Disease. Diabetes. 2015; 64:3464–74. [PubMed: 26153245]
2. Garg SK, Maurer H, Reed K, Selagamsetty R. Diabetes and cancer: two diseases with obesity as a common risk factor. Diabetes Obes Metab. 2014; 16:97–110. [PubMed: 23668396]
3. Giralt M, Villarroya F. White, brown, beige/brite: different adipose cells for different functions? Endocrinology. 2013; 154:2992–3000. [PubMed: 23782940]
4. Wu J, Boström P, Sparks L, Ye L, Choi JH, Giang AH, et al. Beige Adipocytes Are a Distinct Type of Thermogenic Fat Cell in Mouse and Human. Cell. 2012; 150:366–76. [PubMed: 22796012]
5. Saito M, Okamatsuogura Y, Matsushita M, Watanabe K, Yoneshiro T, Niokobayashi J, et al. High Incidence of Metabolically Active Brown Adipose Tissue in Healthy Adult Humans. Diabetes. 2009; 58:1526–31. [PubMed: 19401428]
6. Bonet ML, Oliver P, Palou A. Pharmacological and nutritional agents promoting browning of white adipose tissue. BBA-Mol Cell Biol L. 2013; 1831:969–85.
7. Zhu MJ, Kang Y, Xue Y, Liang X, García MPG, Dan R, et al. Red raspberries suppress NLRP3 inflammasome and attenuate metabolic abnormalities in diet-induced obese mice. J Nutr Biochem. 2018; 53:96–103. [PubMed: 29202274]
8. Luo T, Miranda-Garcia O, Adamson A, Sasaki G, Shay NF. Development of obesity is reduced in high-fat fed mice fed whole raspberries, raspberry juice concentrate, and a combination of the raspberry phytochemicals ellagic acid and raspberry ketone. J Berry Research. 2016; 6:213–23.

9. Noratto GD, Chew BP, Atienza LM. Red raspberry (Rubus idaeus L.) intake decreases oxidative stress in obese diabetic (db/db) mice. Food Chem. 2017; 227:305–14. [PubMed: 28274436]
10. Noratto G, Chew BP, Ivanov I. Red raspberry decreases heart biomarkers of cardiac remodeling associated with oxidative and inflammatory stress in obese diabetic db/db mice. Food Funct. 2016; 7:4944–55. [PubMed: 27841417]
11. Ghalayini IF, Al-Ghazo MA, Harfeil MN. Prophylaxis and therapeutic effects of raspberry (Rubus idaeus) on renal stone formation in Balb/c mice. Int Braz J Urol. 2011; 37:259–67. [PubMed: 21557843]
12. Andrade JMO, Frade ACM, Guimaraes JB, Freitas KM, Lopes MTP, Guimarães ALS, et al. Resveratrol increases brown adipose tissue thermogenesis markers by increasing SIRT1 and energy expenditure and decreasing fat accumulation in adipose tissue of mice fed a standard diet. Euro J Nutr. 2014; 53:1503–10.
13. Wang S, Liang X, Yang Q, Fu X, Rogers C, Zhu M, et al. Resveratrol induces brown-like adipocyte formation in white fat through activation of AMP-activated protein kinase (AMPK) α1. Int J Obesity. 2015; 39:967–76.
14. Hardie DG, Ross FA, Hawley SA. AMPK: a nutrient and energy sensor that maintains energy homeostasis. Nat Rev Mol Cell Bio. 2012; 13:251–62. [PubMed: 22436748]
15. Quentin T, Kitz J, Steinmetz M, Poppe A, Bär K, Krätzner R. Different expression of the catalytic alpha subunits of the AMP activated protein kinase--an immunohistochemical study in human tissue. Histol Histopathol. 2011; 26:589–96. [PubMed: 21432774]
16. Stapleton D, Mitchelhill KI, Gao G, Widmer J, Michell BJ, Teh T, et al. Mammalian AMP-activated Protein Kinase Subfamily. J Biol Chem. 1996; 271:611–4. [PubMed: 8557660]
17. Wang S, Liang X, Yang Q, Fu X, Zhu M, Rodgers B, et al. Resveratrol enhances brown adipocyte formation and function by activating AMP- activated protein kinase (AMPK) α1 in mice fed high-fat diet. Mol Nutr Food Res. 2017; 61:1600746.
18. Hayashi S, Mcmahon AP. Efficient recombination in diverse tissues by a tamoxifen-inducible form of Cre: a tool for temporally regulated gene activation/inactivation in the mouse. Dev Biol. 2002; 244:305–28. [PubMed: 11944939]
19. Fu X, Zhu M, Zhang S, Foretz M, Viollet B, Du M. Obesity impairs skeletal muscle regeneration via inhibition of AMP-activated protein kinase. Diabetes. 2015; 65:188–200. [PubMed: 26384382]
20. Hesselbarth N, Pettinelli C, Gericke M, Berger C, Kunath A, Stumvoll M, et al. Tamoxifen affects glucose and lipid metabolism parameters, causes browning of subcutaneous adipose tissue and transient body composition changes in C57BL/6NTac mice. Biochem Biophys Res Commun. 2015; 464:724–9. [PubMed: 26164229]
21. Yang Q, Liang X, Sun X, Zhang L, Fu X, Rogers CJ, et al. AMPK/α-ketoglutarate axis dynamically mediates DNA demethylation in the Prdm16 promoter and brown adipogenesis. Cell Metab. 2016; 24:542–54. [PubMed: 27641099]
22. Liang X, Yang Q, Fu X, Rogers CJ, Wang B, Pan H, et al. Maternal obesity epigenetically alters visceral fat progenitor cell properties in male offspring mice. J Physiol. 2016; 594:4453–66. [PubMed: 27060371]
23. Harms MJ, Ishibashi J, Wang W, Lim H-W, Goyama S, Sato T, et al. Prdm16 Is Required for the Maintenance of Brown Adipocyte Identity and Function in Adult Mice. Cell Metab. 2014; 19:593–604. [PubMed: 24703692]
24. Zou T, Chen D, Yang Q, Wang B, Zhu MJ, Nathanielsz PW, et al. Resveratrol supplementation to high fat diet-fed pregnant mice promotes brown and beige adipocyte development and prevents obesity in male offspring. J Physiol. 2017; 595:1547–62. [PubMed: 27891610]
25. Livak KJ, Schmittgen TD. Analysis of relative gene expression data using real-time quantitative PCR and the $2^{-\Delta\Delta CT}$ Method. Methods. 2001; 25:402–8. [PubMed: 11846609]
26. Spiegelman BM, Flier JS. Obesity and the regulation of energy balance. Cell. 2001; 104:531–43. [PubMed: 11239410]
27. Symonds ME. Brown Adipose Tissue Growth and Development. Scientifica. 2013; 2013:305763. [PubMed: 24278771]
28. Harms M, Seale P. Brown and beige fat: development, function and therapeutic potential. Nat Med. 2013; 19:1252–63. [PubMed: 24100998]

29. Noratto G, Chew B, Mencia A. Effects of Raspberry Dietary Supplementation on Risk Biomarkers of Diabetes Related Complications and Heart Disease in Diabetic Mice. Faseb J. 2016; 30(1 Supplement):692.23.

30. Carvalho E, Franceschi P, Feller A, Palmieri L, Wehrens R, Martens S. A targeted metabolomics approach to understand differences in flavonoid biosynthesis in red and yellow raspberries. Plant Physiol Biochem. 2013; 72:79–86. [PubMed: 23622736]

31. Schneider K, Valdez J, Nguyen J, Vawter M, Galke B, Kurtz TW, et al. Increased Energy Expenditure, Ucp1 Expression, and Resistance to Diet-induced Obesity in Mice Lacking Nuclear Factor-Erythroid-2-related Transcription Factor-2 (Nrf2). J Biol Chem. 2016; 291:7754–66. [PubMed: 26841864]

32. Ramosjiménez A, Hernándeztorres RP, Torresdurán PV, Romerogonzalez J, Mascher D, Posadasromero C, et al. The Respiratory Exchange Ratio is Associated with Fitness Indicators Both in Trained and Untrained Men: A Possible Application for People with Reduced Exercise Tolerance. Clin Med Circ Respirat Pulm Med. 2008; 2:1–9.

33. Hondares E, Rosell M, Díaz-Delfín J, Olmos Y, Monsalve M, Iglesias R, et al. Peroxisome proliferator-activated receptor α (PPARα) induces PPARγ coactivator 1α (PGC-1α) gene expression and contributes to thermogenic activation of brown fat involvement of PRDM16. J Biol Chem. 2011; 286:43112–22. [PubMed: 22033933]

34. Seale P, Conroe HM, Estall J, Kajimura S, Frontini A, Ishibashi J, et al. Prdm16 determines the thermogenic program of subcutaneous white adipose tissue in mice. J Clin Invest. 2011; 121:96–105. [PubMed: 21123942]

35. Seale P, Bjork B, Yang W, Kajimura S, Chin S, Kuang S, et al. PRDM16 controls a brown fat/skeletal muscle switch. Nature. 2008; 454:961–7. [PubMed: 18719582]

36. Seale P, Kajimura S, Spiegelman BM. Transcriptional control of brown adipocyte development and physiological function—of mice and men. Genes Dev. 2009; 23:788–97. [PubMed: 19339685]

37. McDonald ME, Li C, Bian H, Smith BD, Layne MD, Farmer SR. Myocardin-related transcription factor A regulates conversion of progenitors to beige adipocytes. Cell. 2015; 160:105–18. [PubMed: 25579684]

38. Tharp KM, Jha AK, Kraiczy J, Yesian A, Karateev G, Sinisi R, et al. Matrix-assisted transplantation of functional beige adipose tissue. Diabetes. 2015; 64:3713–24. [PubMed: 26293504]

39. Zhang X, Zhang Q, Wang X, Zhang L, Qu W, Bao B, et al. Dietary luteolin activates browning and thermogenesis in mice through an AMPK/PGC1α pathway-mediated mechanism. Int J Obesity. 2016; 40:1841–9.

40. Lee YH, Petkova AP, Konkar AA, Granneman JG. Cellular origins of cold-induced brown adipocytes in adult mice. Faseb J. 2015; 29:286–99. [PubMed: 25392270]

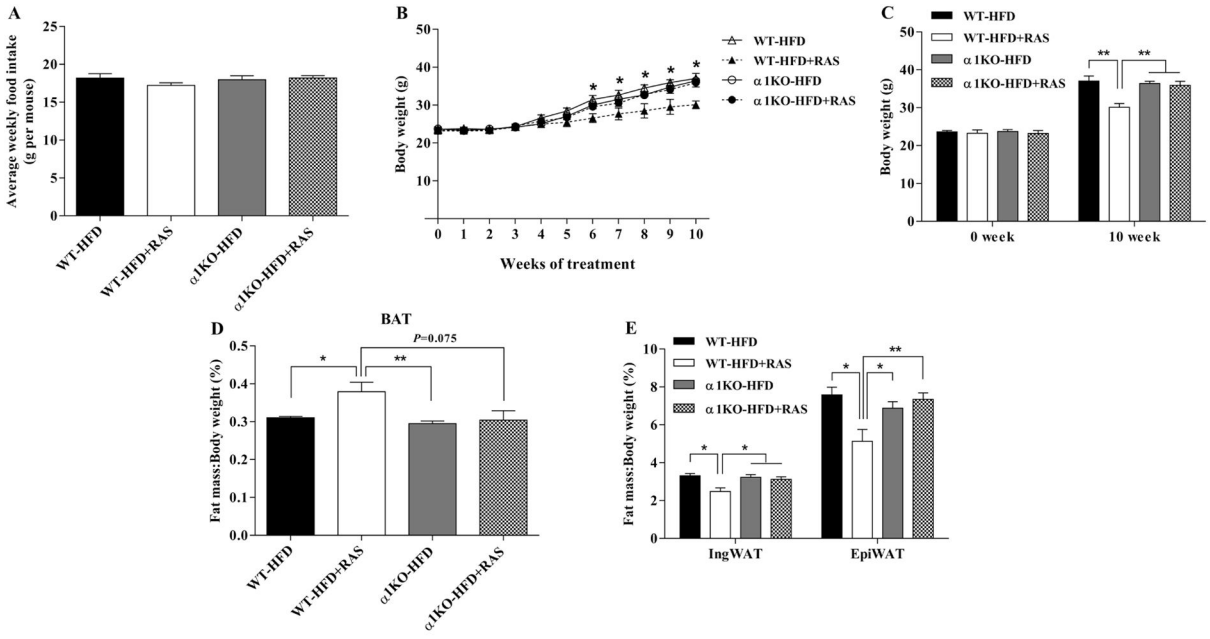

Figure 1. Raspberry does not reduce body weight gain and adiposity in AMPKα1$^{-/-}$ mice challenged with HFD

To achieve AMPKα1 conditional knockout, AMPKα1$^{flox/flox}$ mice (WT) and Rosa^{Cre}/AMPKα1$^{flox/flox}$ (AMPKα1$^{-/-}$, α1KO) mice were injected intraperitoneally with tamoxifen (75 μg/g body weight) for 4 continuous days. Then, mice were fed with HFD with/without 5% raspberry for 10 weeks. *A*, weekly food intake. *B and C*, body weight changes. *D*, ratio of brown adipose tissue to body weight. *E*, ratio of white adipose tissue to body weight. *P < 0.05 and **P < 0.01. Data are expressed as means ± SEM (n = 6).

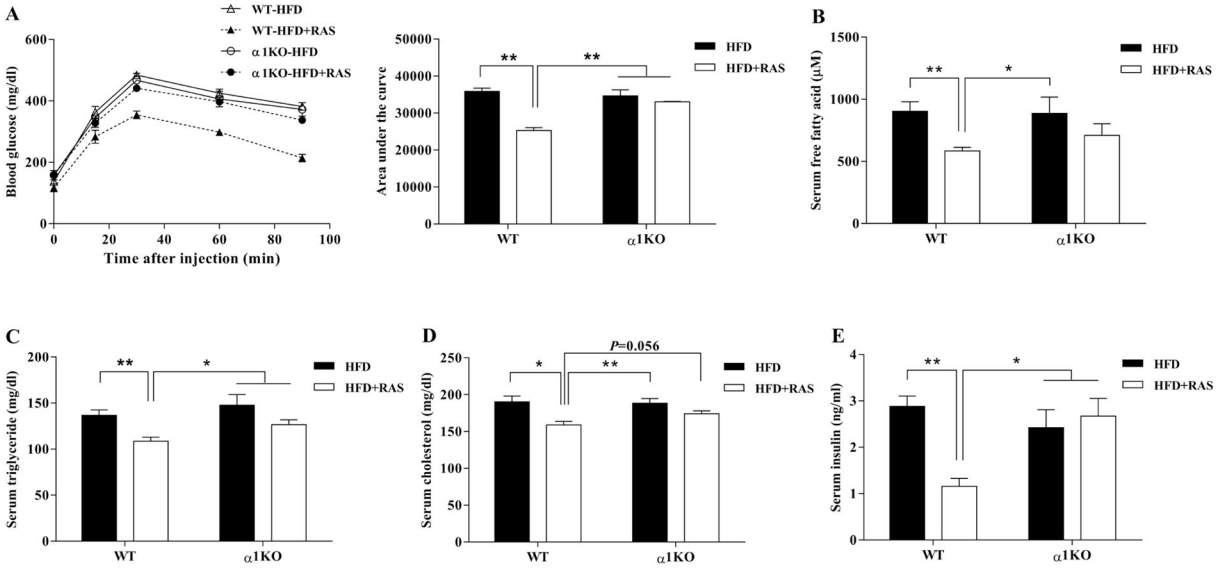

Figure 2. Raspberry does not improve insulin sensitivity in AMPKα1$^{-/-}$ mice challenged with HFD

Mice of both WT and AMPKα1$^{-/-}$ with/without raspberry treatments were subjected to glucose tolerance test at 9 weeks of dietary treatment. *A*, glucose tolerance test and area under the curve. *B*, serum free fatty acid concentrations. *C*, serum triglyceride concentrations. *D*, serum cholesterol concentrations. *E*, serum insulin concentrations. **P* < 0.05 and ***P* < 0.01. Data are expressed as means ± SEM (*n* = 6).

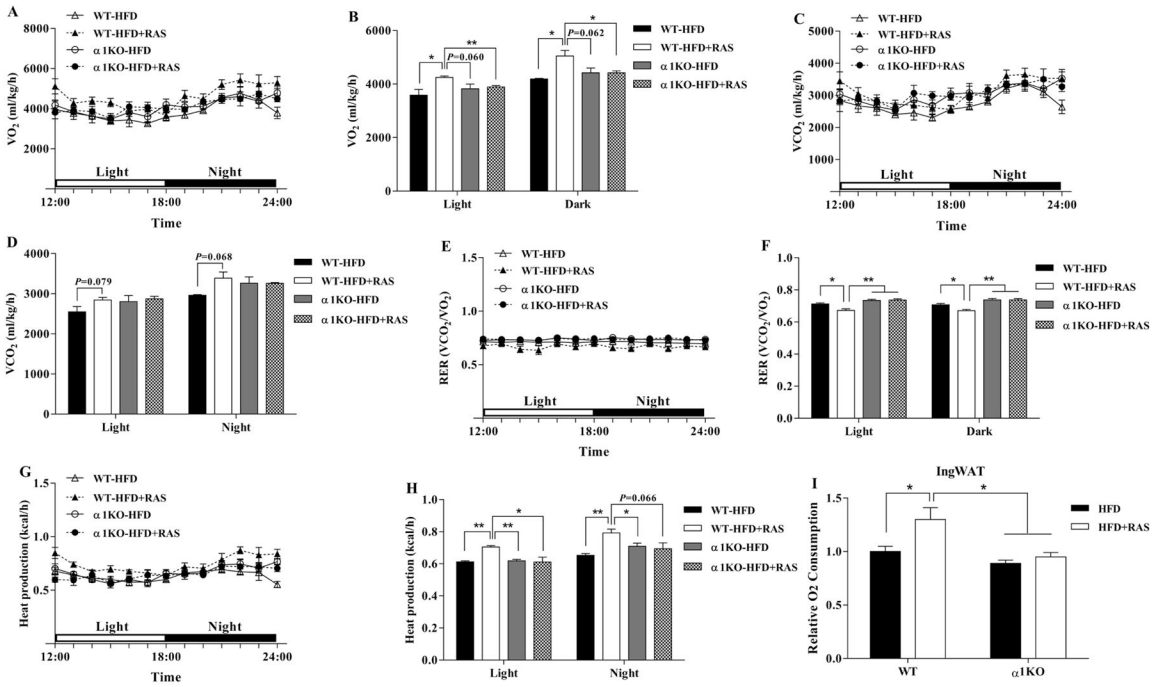

Figure 3. Raspberry does not increase energy expenditure in AMPKα1$^{-/-}$ mice challenged with HFD

A–H, Before necropsy, mice were subjected to the analysis of whole-body metabolic rate [oxygen consumption (VO_2), carbon dioxide production (VCO_2), respiratory exchange ratio (RER) and heat production] during the day (quiescent stage) and night (active stage) using an Oxymax indirect open-circuit calorimetry system (Columbus Instruments, Columbus, OH, USA). VO_2 during a 6 h light-6 h dark cycle measured in a metabolic cage (*A*) and the average values (*B*). VCO_2 during a 6 h light-6 h dark cycle (*C*) and the average values (*D*). The values of RER (ratio of VCO_2 to VO_2) were calculated from metabolic chamber data during a 6 h light-6 h dark cycle. Heat production during a 6 h light-6 h dark cycle (*G*) and the average values (*H*). *I*, IngWAT was isolated right after necropsy and subjected to basal oxygen consumption *in vitro*. $*P < 0.05$ and $**P < 0.01$. Data are expressed as means ± SEM ($n = 6$).

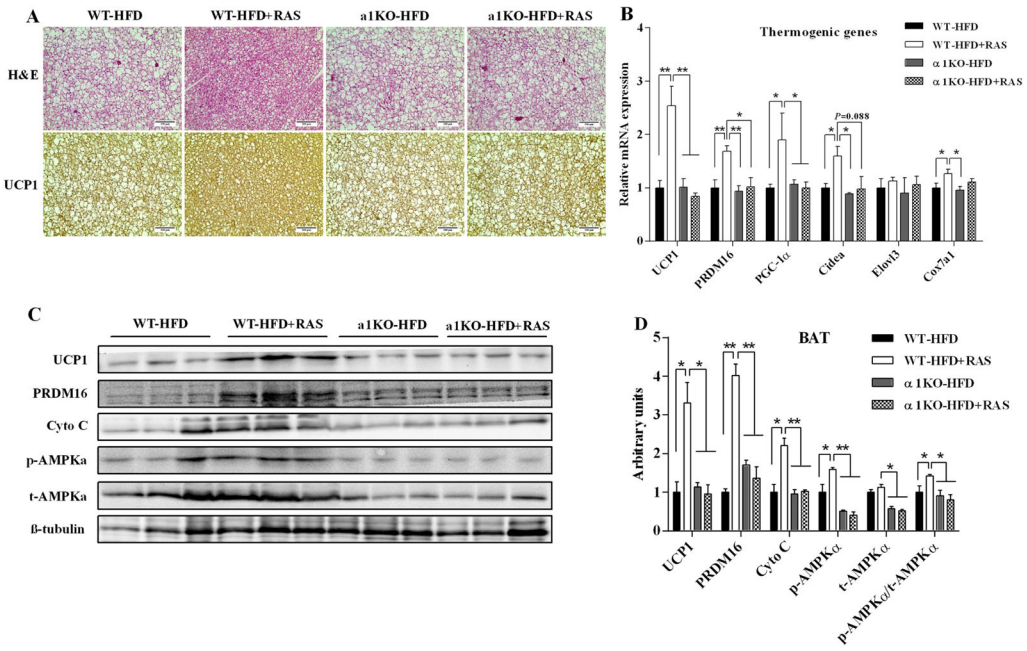

Figure 4. Raspberry does not increase BAT metabolic activity in AMPKα1$^{-/-}$ mice challenged with HFD

AMPKα1$^{flox/flox}$ mice (WT) and Rosa^{Cre}/AMPKα1$^{flox/flox}$ (AMPKα1$^{-/-}$, α1KO) mice were fed with HFD with/without 5% raspberry for 10 weeks, and BAT were sampled for histochemical and biochemical analyses. *A*, representative H&E staining and UCP1 staining for BAT sections. *B*, mRNA expression of thermogenic genes in BAT. *C*, representative images of immunoblotting. *D*, contents of thermogenic proteins and AMPKα. **P* < 0.05 and ***P* < 0.01. Data are expressed as means ± SEM (*n* = 6).

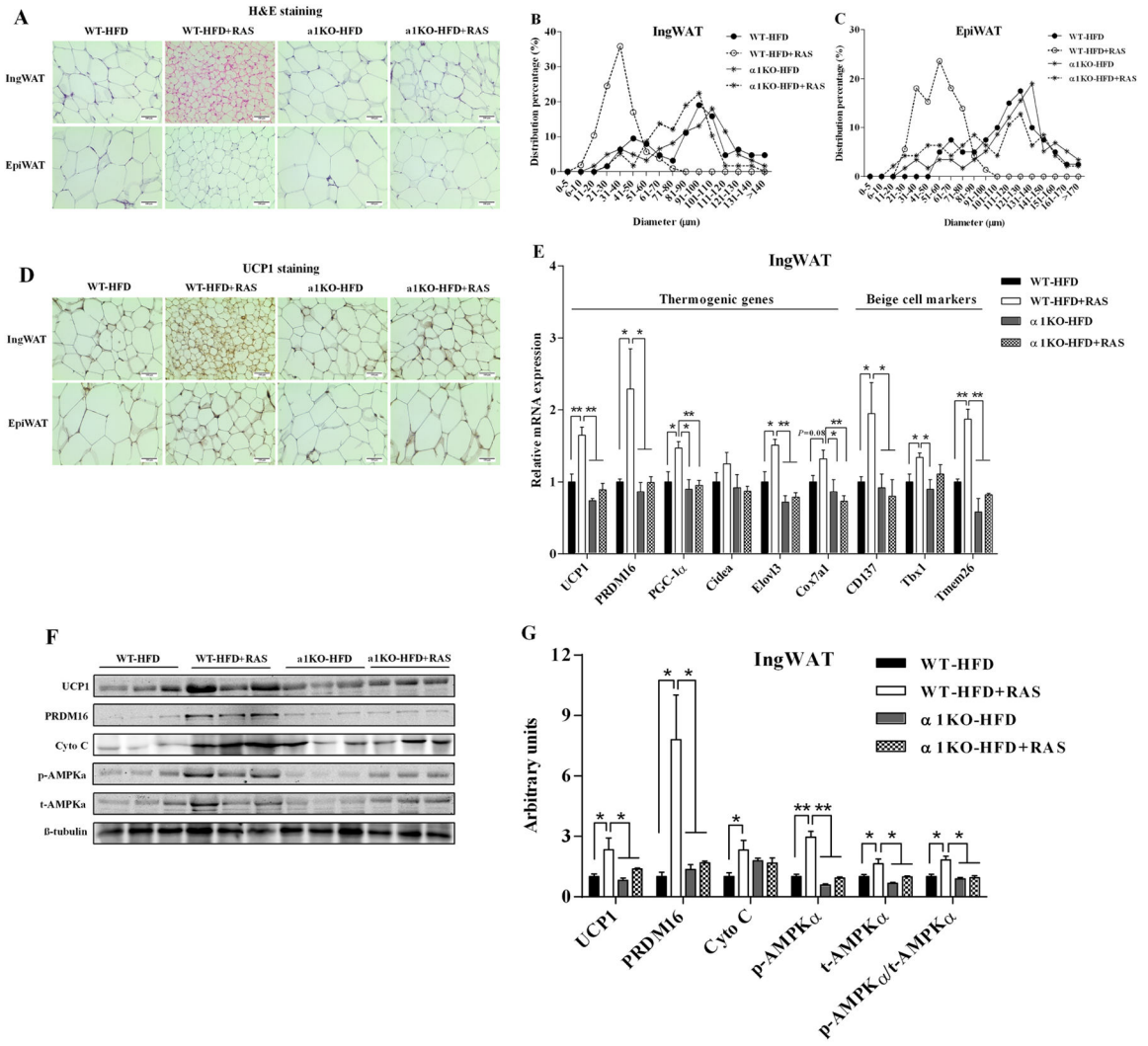

Figure 5. Raspberry does not induce brown fat-like changes in white adipose tissue of AMPKα1$^{-/-}$ mice challenged with HFD

AMPKα1$^{flox/flox}$ mice (WT) and Rosa^{Cre}/AMPKα1$^{flox/flox}$ (AMPKα1$^{-/-}$, α1KO) mice were fed with HFD with/without 5% raspberry for 10 weeks, and IngWAT and EpiWAT were sampled for histochemical and biochemical analyses. *A*, representative H&E staining in IngWAT and EpiWAT sections. *B* and *C*, percentage distribution of adipocyte diameters of IngWAT (*B*) and EpiWAT (*C*). *D*, representative UCP1 staining in IngWAT and EpiWAT sections. *E*, mRNA expression of thermogenic genes and beige adipocyte-selective markers in IngWAT. *F*, representative images of immunoblotting. *G*, contents of thermogenic proteins and AMPKα. $*P < 0.05$ and $**P < 0.01$. Data are expressed as means ± SEM ($n = 6$).

Table 1

Primer sequences used for real-time quantitative PCR

Gene	Forward (5′-3′)	Reverse (5′-3′)	Size (bp)	Access No.
18s	GTAACCCGTTGAACCCCATT	CCATCCAATCGGTAGTAGCG	151	NR_046233.2
UCP1	ACTGCCACACCTCCAGTCATT	CTTTGCCTCACTCAGGATTGG	123	NM_009463.3
PRDM16	CAGCACGGTGAAGCCATTC	GCGTGCATCCGCTTGTG	87	NM_001291029.1
PGC-1α	CCCTGCCATTGTTAAGACC	TGCTGCTGTTCCTGTTTTC	161	XM_006503779.1
Cidea	ATCACAACTGGCCTGGTTACG	TACTACCCGGTGTCCATTTCT	136	NM_007702.2
Elovl3	GATGGTTCTGGGCACCATCTT	CGTTGTTGTGTGGCATCCTT	73	XM_006526624.1
Cox7a1	CAGCGTCATGGTCAGTCTGT	AGAAAACCGTGTGGCAGAGA	112	NM_009944.3
CD137	GTCGACCCTGGACGAACTGCTCT	CCTCTGGAGTCACAGAAATGGTGGTA	132	NM_001077590.1
Tbx1	TGAAGAAGAACCCGAAGGTGG	ACTTGGAACGTGGGGAACATT	133	XM_006536887.1
TMEM26	GAAACCAGTATTGCAGCACCCAAT	AATATTAGCAGGAGTGTTTGGTGGA	205	NM_177794.3